e-ISSN:2582-7219

INTERNATIONAL JOURNAL OF MULTIDISCIPLINARY RESEARCH IN SCIENCE, ENGINEERING AND TECHNOLOGY

Volume 6, Issue 6, June 2023

INTERNATIONAL STANDARD SERIAL NUMBER INDIA

Impact Factor: 7.54

6381 907 438 6381 907 438 ijmrset@gmail.com www.ijmrset.com

International Journal of Multidisciplinary Research in Science, Engineering and Technology (IJMRSET)

| ISSN: 2582-7219 | www.ijmrset.com | Impact Factor: 7.54| Monthly, Peer Reviewed & Referred Journal|

| Volume 6, Issue 6, June 2023 |

| DOI:10.15680/IJMRSET.2023.0606059 |

Computational Methods for Charge Density Waves in 2D Materials

Dr. Kamal Chand Jain

Associate Professor, MLV Textile and Engineering College, Bhilwara, Rajasthan, India

Charge density wave (CDW) is a periodic modulation of electronic charge leading to a reconstruction of the lattice, an emergence of zone folded mode along with collective excitations.[1] Transition metal chalcogenides have shown a great potential to study the underlying physics of multi body interactions like electron-phonon (*e-ph*) as well as plasmons-phonon coupling,[2,3] excitonic complexes[4] and CDW instabilities.[5,6] We are elaborating on the collective excitation and multiphonon interactions like amplitude, zone-folded and two phonon (2_{ph}) mode associated with CDW in 2H-TaS_2 and 2H-$NbSe_2$. The 2_{ph} is a unique excitation appears due to anharmonicity mediated longitudinal acoustic modes associated with the Kohn anomaly and provides a substantial evidences of *e-ph* coupling.[7] The experimental observations of anomalous response of 2_{ph} mode across CDW is clarified with phonon self- energy formalism. Transport measurements shows that both materials exhibit incommensurate CDW (T_{I-CDW}) at ~ 76 K (2H-TaS_2) and ~ 30 K (2H-$NbSe_2$). As revealed by the estimated *e-ph* coupling ($\lambda \sim 0.007$ for 2H-$NbSe_2$ and ~ 0.013 for 2H-TaS_2) and anharmonicity constant ($\delta \sim 6.92$ for 2H-$NbSe_2$ and ~ 2.723 for 2H-TaS_2), we emphasize on higher *e-ph* coupling in 2H-TaS_2 while larger anharmonicity 2H-$NbSe_2$.

Two phonon (*2ph*) modes are the collective excitations associated with the correlation of multiple phonon branches in the materials having charge density wave (CDW) instabilities arising due to the reconstruction of lattice. CDW is a quantum phenomenon, proposed by Peierls in 1955, wherein the periodic modulation of the electronic charge density is accompanied by the lattice distortion and high anharmonicity.[1] Based on the periodicity of the distorted lattice, CDW can be classified as commensurate (C-CDW), and incommensurate (I-CDW) CDW, where the ordering vector ($qCDW$) is an integral and non- integral multiple of the reciprocal lattice vector of the undistorted phase, respectively.[8] In general, the origin of CDW can be explained by Fermi surface nesting (FSN),[1,5] electron-phonon (*e-ph*) coupling,[9] anharmonicity,[7] and saddle-point singularity.[10] In undistorted solid, the energy spectrum of the electrons consists of allowed energy levels separated by an energy band gap at Brillouin zone (BZ) boundary, (Fig.1a), while in the distorted CDW state the lattice modulation folds the BZ with opening of a gap (Δ_{CDW}) at the Fermi level, ($\vec{q} = \pm 2\vec{k}_F$) (Fig.1b).[11] In the zone-folded (ZF) spectrum, the CDW instability executes new quasi-harmonic vibrations forming a condensate of phonons of specific wave vector, $\pm q$, which are named as collective (amplitude/phase) modes.[12] One such collective modes is formed when an incident photon excites an electron-hole pair which couples to an optical phonon through *e-ph* coupling and named as 2_{ph} mode.[11] The Feynman diagram representing the Raman scattering of 2_{ph} mode is shown in Fig.1c.[7] Specifically, the 2_{ph} mode is a second order scattering near $\vec{q}_{CDW} = \frac{2}{3}\Gamma M$ of two acoustic mode with equal and opposite momentum. The scattering lowers the energy of the modes at certain symmetry points of BZ and appears as a discontinuity (called as Kohn anomaly) in the slope of phonon dispersion (Fig.1d), with a frequency approximately half of 2_{ph} mode.[11] The 2_{ph} mode has been observed in graphene,[13] group-IV nitrides[14] and group-V carbides[15] using Raman scattering and also supported by density functional theory. For transition metal dichalcogenides (TMDCs), the Kohn anomaly arise due to the presence of the coupling of *d* electrons of transition metal with phonons.

| ISSN: 2582-7219 | www.ijmrset.com | Impact Factor: 7.54| Monthly, Peer Reviewed & Referred Journal|

| Volume 6, Issue 6, June 2023 |

| DOI:10.15680/IJMRSET.2023.0606059 |

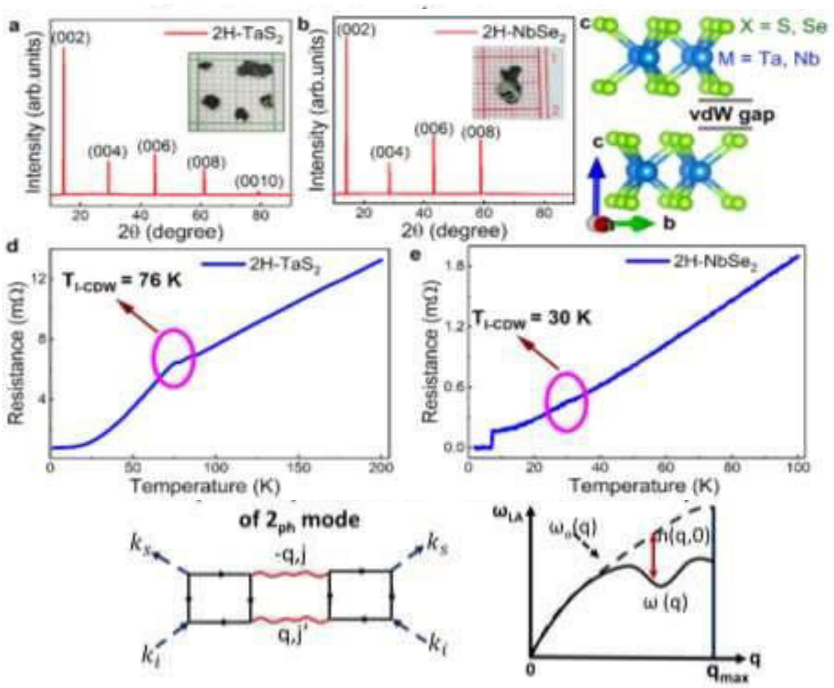

Fig. 1 | Schematic of charge density wave and two-phonon mode. a-b, The atomic arrangement, electronic charge density, and energy band diagram of **a,** undistorted lattice, and **b,** charge density wave state. Modulation of electronic density with change in potential energy of lattice resulting in the opening of band gap (Δ_{CDW}) at fermi level, $q = 2k_F$. **c,** Feynman representation for the Raman scattering of 2_{ph} mode, **d**, The anomalous dispersion curve for longitudinal acoustic (Kohn anomaly) mode with inclusion of all interaction in terms of phonon self-energy ($\pi(q, 0)$ from the *d* electrons of metal atoms.

For TMDCs, while both FSN[1,5] and *e-ph* coupling[9] can drive the CDW yet various experiments like electrical and thermal transport measurement,[16] magnetic measurement,[17] and neutron scattering,[18] and Raman spectroscopy,[9] advocate the *e-ph* coupling as the major cause of CDW instabilities. Previous experimental and theoretical studies such as inelastic neutron and X-ray scattering[18,19], time resolved optical pump-probe spectroscopy[20], density functional calculation[19], on TMDCs showed the softening of the acoustic and 2_{ph} mode with lowering of temperatures until CDW, but the behavior of 2_{ph} mode across CDW is unclear. In this regards, the interpretation of CDW with collective and 2_{ph} mode, especially in case of 2H-NbSe2, 2H-TaSe2,[21] 2H-TaS2,[22] 1T-VSe2[8] is little explored so far.[23] Thus, we report on the involvement of 2_{ph} mode with *e-ph* coupling and unveiling the key fundamental role of 2_{ph} mode on the onset of CDW phase transitions in 2H-TaS2 and 2H-NbSe2, using low temperature and polarized Raman spectroscopy. We emphasized on the multiphonon interactions associated with CDW instabilities using light matter interactions, which are a powerful way to identify the nature of collective excitations, ZF modes as well as 2_{ph} mode.[9,24] The growth and characterization of single crystal 2H-TaS2 and 2H-NbSe2 are elaborated in the methods, below.

Fig. 2| Characterization of single crystal and observation of CDW. X-ray diffraction pattern of single-crystals **a**, 2H-TaS2 and **b**, 2H-NbSe2, (inset show the photograph of the grown crystals) and **c**, crystal structure of the 2H-MX2 (M = Ta, Nb; X = S, Se), temperature dependent resistance ($R(T)$) of **d,** 2H-TaS2 ($TI\text{-}CDW$ at ~ 76K) and **e,** 2H-NbSe2 ($TI\text{-}CDW$ ~ 30 K).

The single crystalline nature of 2H-TaS2 and 2H-NbSe2 (both have space group *P63/mmc*, 194) has been confirmed from X-ray diffraction pattern (Fig. 2a-b), and the miller indices along (*00l*) direction of all peaks indicate the growth along the *c*-axis. The estimated lattice parameter are $a = b = 3.316$ Å and $c = 12.568$ Å (for 2H-TaS2) and $a = b = 3.442$ Å and $c = 12.548$ Å (for 2H-NbSe2), which are in agreement with the reports.[9,25] Figure. 2c shows the hexagonal unit cell of 2H-MX2 with covalently bonded tri-atomic layers (*X-M-X*), where metal (*M* = *Ta* and *Nb*) atoms are sandwiched between two layers of chalcogens (*X* = *S* and *Se*),[26] and the tri-atomic layers are stacked with weak van der Waals gap. Both 2H-

| ISSN: 2582-7219 | www.ijmrset.com | Impact Factor: 7.54| Monthly, Peer Reviewed & Referred Journal|

| Volume 6, Issue 6, June 2023 |

| DOI:10.15680/IJMRSET.2023.0606059 |

TaS2 and 2H-NbSe2 show metallic behavior in the temperature dependent four-probe resistance ($R(T)$) shown in Fig. 2d-e and these materials undergo an I-CDW and the transition temperature (T-$ICDW$) can be identified from the change in slope of electrical transport measurements.[27-29] Thus, characteristic TI-CDW has been observed at ~ 76 K (for 2H-TaS2) and ~ 30 K (for 2H-NbSe2), whereas 2H-NbSe2 also has a superconducting transition, at TSC ~ 7 K, as shown in Fig. 2d-e.

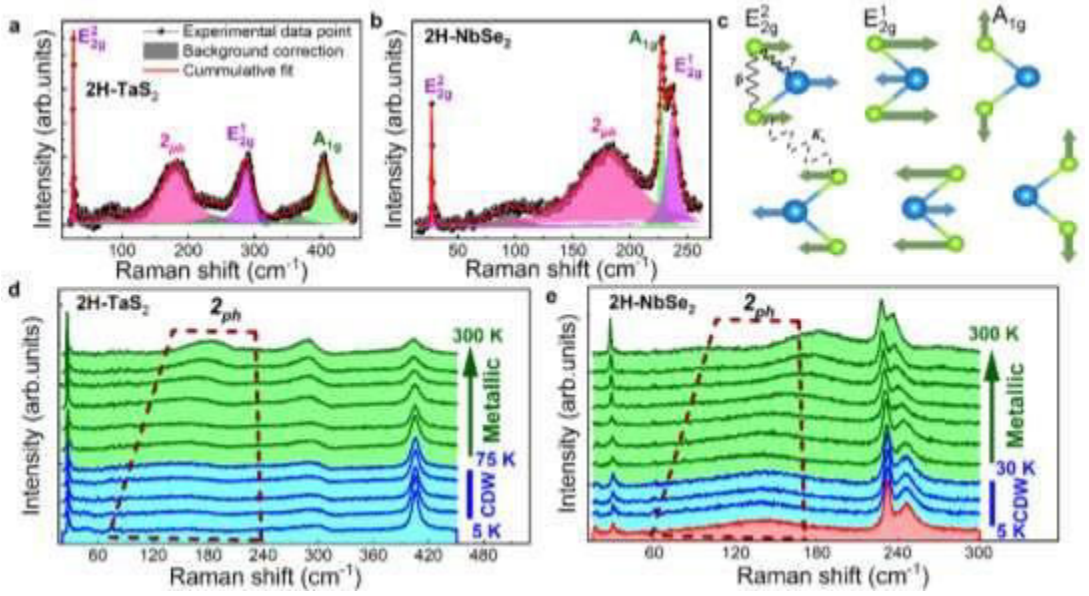

Fig. 3| Raman spectra of 2H-TaS2 and 2H-NbSe2 single crystals. Room temperature Raman spectra of **a,** 2H-TaS2 and **b,** 2H-NbSe2, respectively, and **c,** Schematic of atomic displacements for E^2_{2g}, E^1_{2g} ,

and A_{1g}, Raman modes. Solid black and dashed curved lines represent the intralayer and interlayer spring constant, respectively. Temperature dependent Raman spectra of **d,** 2H-TaS2 and **e,** 2H-NbSe2.

The primitive cell of 2H-MX2 has three atoms, which correspond to nine vibrational modes at the center of the BZ, three of which are acoustic and six are optical. From group theoretical calculations, optical modes can be represented as, $\chi = A_{1g} + E_{1g} + 2E_{2g} + A_{2u} + E_{1u}$, where A_{1g}, E_{1g}, and E_{2g} are Raman active and A_{2u}, and E_{1u} are infra-red active modes[30]. The room temperature Raman spectra for 2H-TaS2 and 2H-NbSe2 are shown in Fig. 3a-b. Here, 2H-TaS2 depicts inter-layer breathing mode (E^2) $_{2g}$

~ 26 cm^{-1}, 2_{ph} mode ~ 182 cm^{-1}, E^1_{2g} ~ 290 cm^{-1} , and A_{1g} ~ 404 cm^{-1} while 2H-NbSe2 have E^2_{2g} ~ 28 cm^{-1}, 2_{ph} mode ~ 184 cm^{-1}, A_{1g} ~ 227 cm^{1} , and E^1 ~ 236 cm^{-1}.[31] The A_{1g} mode involves the out-of-plane vibration (along c-axis) of S/Se atoms against each other whereas E_{2g} mode have in-plane vibrations of Ta (Nb) and S (Se) atoms, and the schematics are presented in Fig. 3c. The other possibilities of Raman active modes have been verified with 633 and 785 nm laser excitations using polarized Raman spectroscopy and are presented in supplementary information (SI) (Fig. S1). The energies of A_{1g} and E_{2g} modes for 2H-TaS2, are higher than 2H-NbSe2 due to stronger ionic bonding arising from higher electronegativity of S atom compared to Se.[32] Besides the characteristic A_{1g} and E_{2g} modes, a broad CDW signature, 2_{ph} mode has also been observed for both 2H-TaS2 and 2H-NbSe2. The detailed analysis of the 2_{ph} mode is done in later texts.

Figure. 3d-e shows the low-temperature Raman spectra for 2H-TaS2 and 2H-NbSe2, respectively. For 2H-NbSe2, the temperature variation of phonon frequency ($\omega(T)$) of both A_{1g} ~ 227 cm^{1} , and E^1 ~ 236 cm^{-1} mode exhibiting hardening because of thermal expansion and anharmonicity (Fig. S2). For 2H- TaS2, the $\omega(T)$ of A_{1g} ~ 404 cm^{-1} mode illustrate anharmonic behavior, while the E^2 ~ 290 cm^{-1} mode show peculiar response (Fig. S2), where negligible shift has been observed down to ~ 100 K, and then hardens with lowering of T, below 100 K.[9] Such an anomalous response of the E^2 mode indicates the signatures of e-ph coupling, associated with the lattice distortion in the CDW phase along the in-plane direction.[9] Further, in line with literatures, various collective modes due to CDW superlattices have also been observed

| ISSN: 2582-7219 | www.ijmrset.com | Impact Factor: 7.54| Monthly, Peer Reviewed & Referred Journal|

| Volume 6, Issue 6, June 2023 |

| DOI:10.15680/IJMRSET.2023.0606059 |

below CDW transition (Fig. S3). In bulk 2H-TaS2, CDW amplitude mode ~ 48 cm^{-1} (E^2), ~ 77 cm^{-1} (A_{1g}), and ZF mode ~ 95 cm^{-1} are observed (Fig. S3a), while 2H-NbSe2 has amplitude mode ~ 38 cm^{-1}, ZF mode ~ 92 cm^{-1}, and a weak mode ~ 190 cm^{-1}, (Fig. S3b) and the origin is unknown so far. The ZF modes of 2H-TaS2 ~ 95 cm^{-1} and 2H-NbSe2 ~ 92 cm^{-1} are positioned at approximately half of the frequency of their respective 2_{ph} mode, and hence, their origin is associated with the Kohn anomaly.

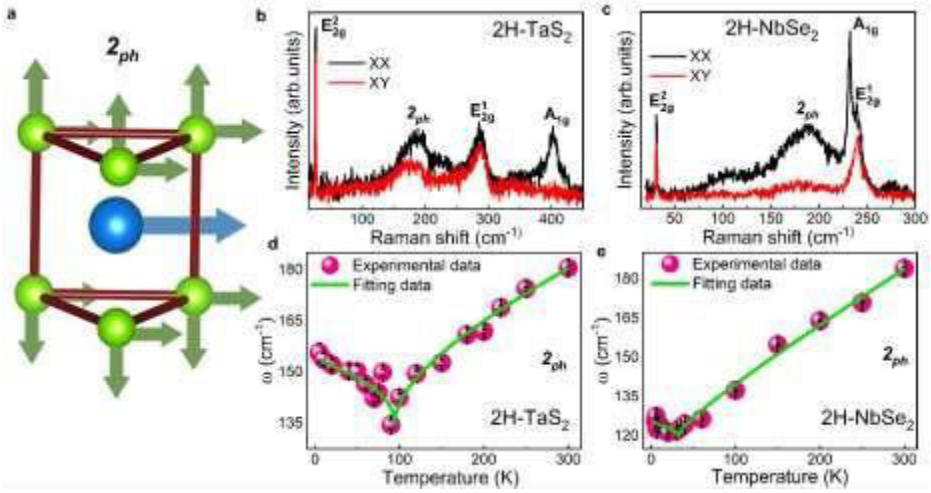

Fig. 4| Involvement of two-phonon mode (2_{ph}) in charge density wave. a, Atomic displacement of Σ_1 symmetry associated with 2_{ph} mode. Polarized Raman spectra of **b,** 2H-TaS2, and **c,** 2H-NbSe2, (*XX* is parallel and *XY* is perpendicular polarization). The anomalous variation of the 2_{ph} mode for **d,** 2H- TaS2 and **e,** 2H-NbSe2, indicates the softening with decreasing temperature until T ~ 100 K and T ~ 30 K, respectively, and subsequent hardening at low temperatures.

The 2_{ph} mode represents a second-order scattering of longitudinal acoustic modes from the other side of the BZ thus exhibits a very low Raman intensity.[33] However, the existence of singularity at $q \sim 2k_F$ in the electronic polarizability can enhance the intensity comparable to characteristic modes. The 2_{ph} mode in 2H-TaSe2,[34] 2H-NbSe2,[34] and 2H-NbS2[35] have a unique Σ_1 symmetry, which predominantly arises because of longitudinal vibration of chalcogen and metal atoms.[18] The schematic of Σ_1 symmetry of 2_{ph} mode is presented in Fig. 4a, where the in-plane displacements of metal atom are larger than chalcogen atom.[34] The involvement of both longitudinal and transverse displacements of 2_{ph} mode have been further confirmed by the polarized Raman spectroscopy using 532 nm laser, at 300K (Fig. 4b-c), where A_{1g} mode

disappeared in *XY* configuration, while 2_{ph} mode with reduced intensity is discernible. The excitation energy dependence of the longitudinal vibrations of 2_{ph} mode have also been confirmed in polarized Raman spectra (*XY* configuration) using 633 and 785 nm lasers (Fig. S1). Therefore, we believe that 2_{ph} mode involve predominant longitudinal vibration of atoms and have a strong influence on the CDW superlattice forms in the basal plane of the hexagonal BZ.[7]

The 2_{ph} mode shows anomalous softening with cooling before the onset of *TI-CDW* for 2H-NbSe2 and hardens later (Fig. 4d-e), on the other hand for 2H-TaS2, the CDW stabilities can exists even at higher temperatures,[9] which is realized from diminished softening at ~ 100 K. The anomalous softening and hardening of 2_{ph} mode below *TI-CDW* arising due to the anharmonicity along with interaction of phonon with the *d* electron of *Ta* and *Nb*.[34] We have fitted the $\omega(T)$ of the 2_{ph} mode for both 2H-TaS2 (Fig. 4d) and 2H-NbSe2 (Fig. 4e), by mean field theory considering a combination of (i) Klemens model for normal mode and (ii) second-order soft mode theory by Tsang.[36] With inclusion of momentum conservations, the combination can be described

$$\Delta\omega(T) = \omega_0 - \delta\left(\frac{2}{e^{\hbar\omega_0/2k_BT}-1}\right) + \lambda\omega'\left|T - T_{cf}\right|^{\frac{1}{2}}, \text{ where } \omega_0 \text{ (at } \sim 0\text{K) and}$$

| ISSN: 2582-7219 | www.ijmrset.com | Impact Factor: 7.54| Monthly, Peer Reviewed & Referred Journal|

| Volume 6, Issue 6, June 2023 |

| DOI:10.15680/IJMRSET.2023.0606059 |

ω' (at high temperatures) of 2_{ph} mode, δ is an anharmonic constant (depends on phonon dispersion), λ is *e-ph* coupling constant and T_{cf} is the transition temperature of instabilties.[36] The experimental data are well fitted with equation and are showing a significant softening down to ~ 100 K (2H-TaS_2) and ~ 30 K (2H-$NbSe_2$), respectively. Here, the value of ω' is fixed and the extracted parameters are tabulated in Table S1. of SI. For 2H-$NbSe_2$, the T_{cf} ~ 32 K is approximately equivalent to $T_{I\text{-}CDW}$ ~ 30 K, whereas T_{cf} of 2H-TaS_2 is ~ 100 K, which is higher than the $T_{I\text{-}CDW}$ ~ 76 K showing the involvements of instabilities. The high T_{cf} indicates that CDW instability in 2H-TaS_2 can persists above the actual $T_{I\text{-}CDW}$ (~ 76 K), which is also established by the anomalous $\omega(T)$ of E^2_{2g} mode (Fig. S2). The observation of high T_{cf} 2_{ph} mode for 2H-TaS_2 has also been shown by the time-resolved optical pump-probe spectroscopy and density functional theory, which predict the existence of non-BCS like transition at ~ 100 K.[7,20] The bulk 2H-TaS_2 have δ ~ 2.723 and λ ~ 0.013, whereas 2H-$NbSe_2$ have δ ~ 6.92 and λ ~ 0.007, which is indicating that both materials have significant amount of anharmonic interactions. On comparing the value of λ, it has been observed that strength of *e-ph* coupling is stronger in case of 2H-TaS_2 than 2H-$NbSe_2$ leading to persistence of CDW instability in 2H-TaS_2 at higher temperature (~ 100 K). Unlike to the earlier reports on inelastic X-ray scattering of 2H-$NbSe_2$[19] and VSe_2[37], where the longitudinal acoustic mode have been collapsed in the CDW region whereas we have observed an anomalous hardening for 2_{ph} mode of 2H-TaS_2 and 2H-$NbSe_2$. Our study illustrates phonon hardening below $T_{I\text{-}CDW}$, which can be incorporated with the numerical formalism of phonon self-energy in the presence of anharmonic interaction and *e-ph* coupling.[7,11](Section.4 in SI) The anomalous ω (T) and full-width at half-maximum (β) of 2_{ph} mode, (Fig. S4a) increase till ~ 100 K and then decreases. Such an anomalous behavior of 2_{ph} mode arises from the coupling of phonons with *d* electrons near the fermi energy and due to the anharmonic interaction.[11,19] Thus, not only the collective modes the anharmonic mediated 2_{ph} mode plays a key role in understanding of CDW superlattices of 2H-polytypes of 2H-TaS_2 and 2H-$NbSe_2$.

In summary, the origin, symmetry, and key role of multiphonon interactions (collective amplitude and anharmonic-mediated 2_{ph} mode) across the CDW instability are emphasized for 2H-TaS_2 and 2H- $NbSe_2$. The low temperature polarized Raman results provide considerable evidence for the existence of CDW instability in 2H-TaS_2 even up to 100 K, which is high as compared to the $T_{I\text{-}CDW}$ ~ 76 K. The observations clarified the involvement of longitudinal vibration of atoms associated with 2_{ph} mode and key evidence of *e-ph* coupling with anharmonicity during reconstruction of the CDW lattices.

I. METHODS

Single crystal of 2H-$NbSe_2$ and 2H-TaS_2 were grown by chemical vapor transport technique using iodine as a transporting agent.[38] X-ray diffraction of the grown single crystal was obtained using a rotating anode Rigaku SmartLab diffractometer in Bragg-Brentano with CuK_α radiation (λ = 1.5406 Å). Low temperature resistance measurement was performed by four probe method in the temperature range of 3 to 300 K using a Quantum Design make physical properties measurement system. Raman scattering measurements were performed using Horiba Jobin-Vyon LabRAM HR Evolution Raman spectrometer with Czerny-turner grating (1800 gr/mm) and Peltier cooled CCD detector in a back-scattering configuration. The 532 nm, 633 nm, and 785 nm lasers were used to excite the sample and 50X long working distance objective lens was used to focus on the crystal. Ultra-low frequency filters were used to access low-frequency Raman modes. To control the polarization, a $\lambda/2$ half-waveplate and an analyzer have been used before the objective lens and spectrometer respectively to select the desired polarization of the incident and scattered light. Temperature-dependent Raman measurements were performed in the temperature range of 3-300K using a Montana instrument make closed-cycle cryostat. All the Raman spectra were fitted by Lorentzian function to evaluate full width at half-maximum (β), frequency (ω), and intensity (I) of Raman modes.

Data availability: All other data supporting the findings of this study are available upon request from the corresponding author.

REFERENCES

1 Grüner, G. The dynamics of charge-density waves. *Rev.of Mod.Phys.* **60**, 1129-1181 (1988).

2 Pandey, J. *et al.* Raman Spectroscopy Study of Phonon Liquid Electron Crystal in Copper Deficient Superionic Thermoelectric $Cu_{2-x}Te$. *ACS Appl. Ener. Mat.* **3**, 2175-2181 (2020).

3 Rawat, D., Singh, A., Singh, N. K. & Soni, A. Anisotropic light-matter interactions in the single-crystal topological insulator bismuth selenide. *Phys. Rev. B* **107**, 155203 (2023).

| ISSN: 2582-7219 | www.ijmrset.com | Impact Factor: 7.54| Monthly, Peer Reviewed & Referred Journal|

| Volume 6, Issue 6, June 2023 |

| DOI:10.15680/IJMRSET.2023.0606059 |

4 Pandey, J. & Soni, A. Unraveling biexciton and excitonic excited states from defect bound states in monolayer MoS_2. *Appl. Surf. Sci.* **463**, 52-57 (2019).
5 Wilson, J., Di Salvo, F. & Mahajan, S. Charge-density waves in metallic, layered, transition-metal dichalcogenides. *Phys. Rev. Lett.* **32**, 882 (1974).
6 Rawat, D., Thomas, A. & Soni, A. Symmetry breaking and structure instability in ultra-thin 2H-TaS_2 across charge density wave transition *arXiv:2307.08418 (Submitted)* (2023).
7 Behera, S. N. & Mohanty, G. C. Theory of two-phonon modes in layered charge-density-wave systems. *Pramana* **26**, 239-261 (1986).
8 Pandey, J. & Soni, A. Electron-phonon interactions and two-phonon modes associated with charge density wave in single crystalline VSe_2. *Phys. Rev. Res.* **2**, 033118 (2020).
9 Joshi, J. *et al.* Short-range charge density wave order in 2H-TaS_2. *Phys. Rev. B* **99**, 245144 (2019).
10 Rice, T. M. & Scott, G. K. New Mechanism for a Charge-Density-Wave Instability. *Phys. Rev. Lett.* **35**, 120-123 (1975).
11 Klein, M. Theory of two-phonon Raman scattering in transition metals and compounds. *Phys. Rev. B* **24**, 4208 (1981).
12 Hansen, M. O. *et al.* Collective modes in the charge density wave state of $K_{0.3}MoO_3$: Role of long-range Coulomb interactions revisited. *Phy. Rev. B* **108**, 045148 (2023).
13 Popov, V. N. Two-phonon Raman bands of bilayer graphene: Revisited. *Carbon* **91**, 436-444 (2015).
14 Spengler, W. & Kaiser, R. First and second order Raman scattering in transition metal compounds. *Solid State Commun.* **18**, 881-884 (1976).
15 Wipf, H., Klein, M. V. & Williams, W. S. Vacancy-Induced and Two-Phonon Raman Scattering in ZrC_x, NbC_x, HfC_x, and TaC_x. *Basic Solid State Phys.* **108**, 489-500 (1981).
16 Gupta, R., Rajeev, K. & Hossain, Z. J. J. o. P. C. M. Thermal transport studies on charge density wave materials $LaPt_2Si_2$ and $PrPt_2Si_2$. *Journ. of Phys.: Cond. Matt.* **30**, 475603 (2018).
17 Lavagnini, M. *et al.* Evidence for coupling between charge density waves and phonons in two-dimensional rare-earth tritellurides. *Phys. Rev. B* **78**, 201101 (2008).
18 Moncton, D. E., Axe, J. D. & Disalvo, F. J. Neutron scattering study of the charge-density wave transitions in 2H-$TaSe_2$ and 2H-$NbSe_2$. *Phys. Rev. B* **16**, 801 (1977).
19 Weber, F. *et al.* Extended Phonon Collapse and the Origin of the Charge-Density Wave in 2H-$NbSe_2$. *Phys. Rev. Lett.* **107**, 107403 (2011).
20 Anikin, A. *et al.* Ultrafast dynamics in the high-symmetry and in the charge density wave phase of 2H-$NbSe_2$. *Phys. Rev. B* **102**, 205139 (2020).
21 Hajiyev, P., Cong, C., Qiu, C. & Yu, T. Contrast and Raman spectroscopy study of single- and few-layered charge density wave material: 2H-$TaSe_2$. *Sci. Rep.* **3**, 2593 (2013).

INTERNATIONAL STANDARD SERIAL NUMBER INDIA

INTERNATIONAL JOURNAL OF MULTIDISCIPLINARY RESEARCH

IN SCIENCE, ENGINEERING AND TECHNOLOGY

| Mobile No: +91-6381907438 | Whatsapp: +91-6381907438 | ijmrset@gmail.com |

www.ijmrset.com